*Transactions*, SMiRT-23
Manchester, United Kingdom - August 10-14, 2015
Division II, Paper ID 287

Fracture Mechanics and Structural Integrity

# DEVELOPMENT OF TEST GUIDANCE FOR COMPACT TENSION FRACTURE TOUGHNESS SPECIMENS CONTAINING NOTCHES INSTEAD OF FATIGUE PRE-CRACKS

**Anthony Horn[1], Peter Budden[2]**

[1] Structural Integrity Specialist, Amec Foster Wheeler, UK.
[2] R6 Lead Engineer, EDF Energy, UK.

## ABSTRACT

Structural integrity assessment codes such as R6 and BS7910 provide guidance on the assessment of flaws that are assumed to be infinitely sharp. In many cases, such as fatigue cracks, this assumption is appropriate; however it can be pessimistic for flaws that do not have sharp tips such as lack of fusion, porosity or mechanical damage. Several methods have been proposed in the literature to quantify the additional margins that may be present for non-sharp defects compared to the margins that would be calculated if the defect were assumed to be a sharp crack. A common feature of these methods is the need to understand how the effective toughness, characterised using the J-integral for a notch, varies with notch acuity. No comprehensive guidance currently exists for obtaining J experimentally from specimens containing notches; hence the typical approach is to use equations intended for pre-cracked specimens to calculate J for notched specimens.

This paper presents a comprehensive set of test guidance for calculating J from Compact Tension (CT) fracture toughness specimens containing notches instead of fatigue pre-cracks. This has been achieved using 3D Finite Element Analyses to quantify the accuracy of formulae intended for pre-cracked specimens in fracture toughness testing standards ASTM E1820, BS7448-1 and ESIS P2-92 when applied to specimens containing notches. The paper quantifies the accuracy of these equations for notched CT specimens and identifies the conditions under which the equations can lead to inaccurate measurement of J for notched specimens.

## INTRODUCTION

Structural integrity assessment codes such as R6 (EDF Energy, 2015) and BS7910 (BSI, 2013) currently provide guidance on the assessment of flaws that are assumed to be infinitely sharp using the Failure Assessment Diagram (FAD). In many cases, such as fatigue cracks, the assumption that the defect tip is infinitely sharp is appropriate. However, this assumption is pessimistic for flaws that do not have sharp tips such as lack of fusion, porosity or mechanical damage. Furthermore, some design features, such as crevices in tube to tubeplate assemblies, are usually treated as crack-like defects in assessments, which could be excessively pessimistic. The current philosophy is to assume all flaws have infinitely sharp tips, thereby ensuring that flaws without sharp tips are assessed pessimistically.

Several methods have been proposed in the literature to quantify the additional margins that may be present for non-sharp defects compared to the margins that would be calculated if the defect were assumed to be a sharp crack. A common feature of these methods is the need to understand how the effective toughness, characterised using the J-integral for a notch, varies with notch acuity. No comprehensive guidance currently exists for obtaining J experimentally from specimens containing notches; hence the typical approach is to use equations intended for pre-cracked specimens to calculate J for notched specimens. The aim of the work presented in this paper is to develop test guidance for Compact Tension (CT) specimens containing notches instead of fatigue pre-cracks. Test guidance for

Single Edge Notch Bend (SENB) specimens containing notches has also been developed recently and is reported separately (Horn and Budden, 2015).

***Test Procedures for Pre-Cracked CT Specimens***

The standard procedure for measuring J using pre-cracked CT specimens involves the use of a stepped-notch design with width W, thickness B, and crack depth a as shown in Figure 1. The specimen design enables Load Line Displacement (LLD) to be measured between knife edges placed at the notch mouth between the pin holes. For the CT specimen, LLD is equal to the Crack Mouth Opening Displacement (CMOD). For consistency with testing standards, when referring to displacement measurement for CT specimens, the term LLD rather than CMOD is used in this paper.

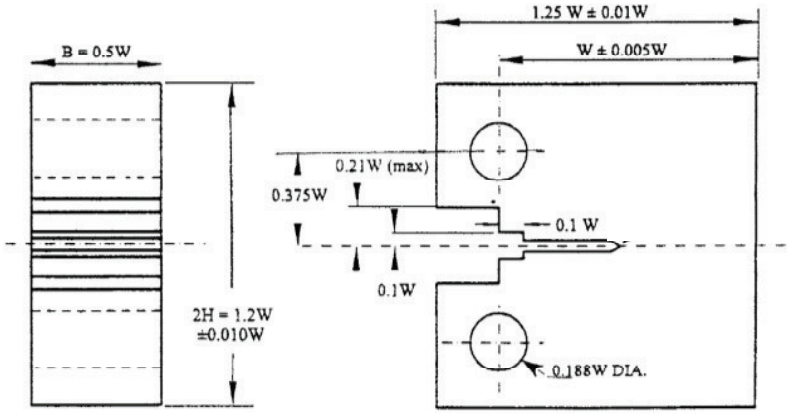


Figure 1: Stepped-notch Compact Tension (CT) specimen, from ASTM E1820-11 (ASTM, 2011)

***Calculation Of J For Pre-Cracked Specimens***

Two general types of expression are available for obtaining J from pre-cracked CT specimens, both of which are based on the area under the load vs. displacement curve. The first expression is based on the total area and is the method specified in ESIS P2-92 (ESIS, 1992):

$$J_{ESIS} = \frac{\eta U}{B(W-a)} \tag{1}$$

where $\eta = 2 + 0.522(1 - a/W)$ and U = total area under the load vs. LLD curve. The second expression partitions J into elastic and plastic components and is the method specified in both ASTM E1820 (ASTM, 2011) and BS7448-1 (BSI, 1991):

$$J_{ASTM} = J_e + J_p = \frac{K^2(1-\nu^2)}{E} + \frac{\eta_p U_p}{B(W-a)} \tag{2}$$

where $J_e$ = elastic component of J
$J_p$ = plastic component of J
K = the linear elastic stress intensity factor as defined in ASTM E1820 and BS7448-1
$\nu$ = Poisson's ratio
E = elastic modulus
$\eta_p = 2 + 0.522(1 - a/W)$ in both ASTM E1820 and BS7448-1
$U_p$ = plastic component of the area under load vs. displacement curve

## DEVELOPMENT OF TEST GUIDANCE FOR NOTCHED CT SPECIMENS

No comprehensive guidance currently exists for obtaining J experimentally from notched CT specimens. The objective of this section of the paper is to evaluate the accuracy of existing equations intended for pre-cracked CT specimens for predicting J of CT specimens containing notches, and to propose new equations if required. For the analysis of CT specimens, expressions for J using both the non-partitioned ESIS expression (Equation 1) and the partitioned ASTM expression (Equation 2) have been compared with the J-integral obtained using Finite Element (FE) analysis, using the methodology described below.

## METHODOLOGY

### *Finite Element Analysis*

Three-dimensional, small-strain, elastic-plastic, FE analyses were used to simulate CT specimens containing sharp cracks and blunt notches loaded in tension. Fifteen models were constructed such that a range of notch root radii values, ρ, could be studied and potential size effects investigated. The overall matrix of geometries modelled is shown in Table 1. The geometrical parameters were chosen to match those of test data that were available for validation purposes, and a/W=0.5 in each case.

Table 1: Matrix of FE models of CT specimens

| B (mm) | W (mm) | a (mm) * | ρ (mm) | ρ/a |
|---|---|---|---|---|
| 6.25 | 12.5 | 6.25 | 0.0025 | 0.0004 |
| | | | 0.16 | 0.0256 |
| | | | 0.25 | 0.04 |
| | | | 0.50 | 0.08 |
| | | | 1.00 | 0.16 |
| 12.5 | 25 | 12.5 | 0.005 | 0.0004 |
| | | | 0.32 | 0.0256 |
| | | | 0.50 | 0.04 |
| | | | 1.00 | 0.08 |
| | | | 2.00 | 0.16 |
| 25 | 50 | 25 | 0.01 | 0.0004 |
| | | | 0.64 | 0.0256 |
| | | | 1.00 | 0.04 |
| | | | 2.00 | 0.08 |
| | | | 4.00 | 0.16 |

** the notch depth a is measured to the tip of the notch*

The CT models containing notches of ρ/a=0.0256 and 0.16 are shown in Figure 2. Specimens with ρ/a ratios greater than 0.16 were not modelled due to the proximity of the notch flanks to the loading hole. It is also unlikely that such specimens could be tested in practice because there would be insufficient material remaining to machine a step on the notch flank from which LLD could be measured. The fatigue pre-cracked specimens were modelled with a small notch root radius (ρ/a=0.0004) to allow for consistency of mesh design between the pre-cracked and notched specimens.

Plasticity was modelled using a Ramberg-Osgood fit to true-stress vs. true-strain curves obtained from tensile tests on a modified grade S690 structural steel reported in Horn and Sherry (2010) where the strain hardening exponent n=6.5. All analyses were performed using ABAQUS version 6.12-1.

Symmetry conditions were specified along the uncracked ligament ($x_2$=0) and the longitudinal mid-plane ($x_3$=B/2) thereby enabling one quarter of each CT specimen to be modelled numerically. Each model consisted of linear 8-noded full integration hexahedral elements (C3D8) arranged into 14 variable thickness layers. The thickest element layer was defined at the longitudinal mid-plane with thinner elements defined near the free surface to accommodate the reduced constraint approaching plane stress conditions. Each model, including the pre-cracked CT specimen, had a straight crack/notch front.

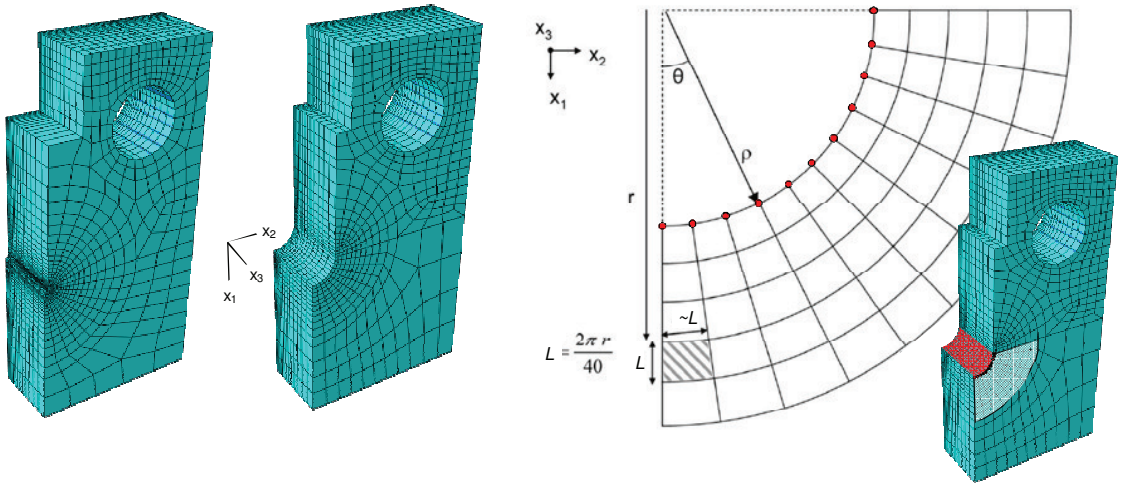


Figure 2: One quarter models of CT specimens with ρ/a=0.0256 and 0.16, and notch tip mesh detail.

Within each of the 14 variable thickness layers, rings of elements enclosed the notch tip as shown in Figure 2 and consistent with the modelling approach described in Horn and Sherry (2012). The notch tip elements had a dimension L in the $x_1$ direction and a dimension approximately equal to L in the angular direction, $\theta=\tan^{-1}(x_2/x_1)$. In the angular direction, 10 equally sized elements were defined in the range $0 \leq \theta \leq \pi/2$ and L was constant with θ. In the $x_1$ direction, L increased with increasing distance r from the centre of curvature of the notch tip, where $L=2\pi r/40$. The ratio ρ/L at r=ρ was therefore the same in all models, including the pre-cracked CT specimen modelled with a finite radius ρ/a=0.0004. This ensured a consistency of mesh structure between models with notches of differing radii.

The loading pin was modelled using a three-dimensional rigid analytical part in the shape of a cylinder positioned within the hole of the CT specimen. Loading in tension was simulated by applying a prescribed displacement in the $x_2$ direction to a single reference point tied to the loading pin. This allowed for measurement of the reaction force through the single reference point. Rotation of the loading pin was prevented by setting all degrees of freedom of the reference point, other than the displacement in the $x_2$ direction, to zero.

### *Calculation Of J*

Small strain FE analyses were used to evaluate the J-integral from the FE models. Small strain analyses were performed because path dependence of the J-integral is less pronounced than for a finite strain analysis as described by Brocks and Scheider (2003). Notch tip stress and strain fields, which would be more accurately modelled using finite strain analyses, were not required as part of the current work. The J-integral was evaluated on contours that completely enclose the notch root: the nodes highlighted in red in Figure 2 define the first contour used to evaluate an individual J-integral value. In the 3D ABAQUS models, the crack front was defined as the surface shaded in red in Figure 2. J-integral values at the specimen centre were almost completely path independent: using the bluntest notch modelled ($\rho/a=0.16$) as an example, all individual J-integral values evaluated on the first 11 contours were within 0.25% of the mean J-integral value for the first 11 contours. At the specimen surface a minor path dependency was observed: the maximum deviation of an individual J-integral value was 5% of the mean J-integral value for the first 11 contours. This minor path dependency was confined to the surface region: just below the surface (4% of the specimen thickness), the J integrals exhibited path independence similar to that observed at the specimen centre.

For each increment of the analysis, an averaged J-integral value, denoted $J_{ave}$, was calculated by taking a weighted average of 15 individual J-integral values evaluated along the notch front. The average was weighted to account for the different element side lengths in the calculation of $J_{ave}$.

Values of $J_{ESIS}$ and $J_{ASTM}$ were calculated from the load vs. LLD curve according to the non-partitioned and partitioned expressions (Equations 1 and 2) respectively. Although the nomenclature $J_{ASTM}$ is used here, it should be noted that $J_{ASTM}$ is identical to $J_{BSI}$ due to the same definition of $\eta_p$ in Equation 2. To apply these equations, LLD was obtained from nodal displacements in the FE models at the crack mouth and in line with the centre of the loading hole. The ratio of both $J_{ESIS}$ and $J_{ASTM}$ to $J_{ave}$ was then calculated at all increments in the FE analysis.

## RESULTS AND DISCUSSION

### *Non-Partitioned Solution ($J_{ESIS}$)*

Figure 3(a) shows the ratio of $J_{ESIS}$ to $J_{ave}$ for the CT specimen plotted as a function of normalised loading level, defined by $J_{ave}/b\sigma_y$, where $b = W-a$ and $\sigma_y$ is the engineering definition of yield stress defined at 0.2% plastic strain. Figure 3(b) shows the ratio of $J_{ESIS}$ to $J_{ave}$ plotted as a function of $\rho/a$ for three levels of normalised $J_{ave}$ denoted by the vertical dashed lines in Figure 3(a). The $J_{ESIS}$ expression can under- and over-predict $J_{ave}$ by up to 15% and 6% respectively, depending on the loading level. However, the results indicate that this variation occurs irrespective of $\rho/a$. The results in both figures indicate that $\rho/a$ has a very small effect on the accuracy of $J_{ESIS}$ for estimating $J_{ave}$. The use of the $J_{ESIS}$ expression, Equation 1, therefore provides a reasonably accurate method for estimating $J_{ave}$ of CT specimens containing notches up to a value of $\rho/a=0.16$, and no worse than that for pre-cracked specimens.

The FE results from all three CT specimen sizes shown in Table 1 were coincident with each other when plotted in non-dimensional form, such as that shown in Figure 3. This confirms that the method used to non-dimensionalise the axes is appropriate.

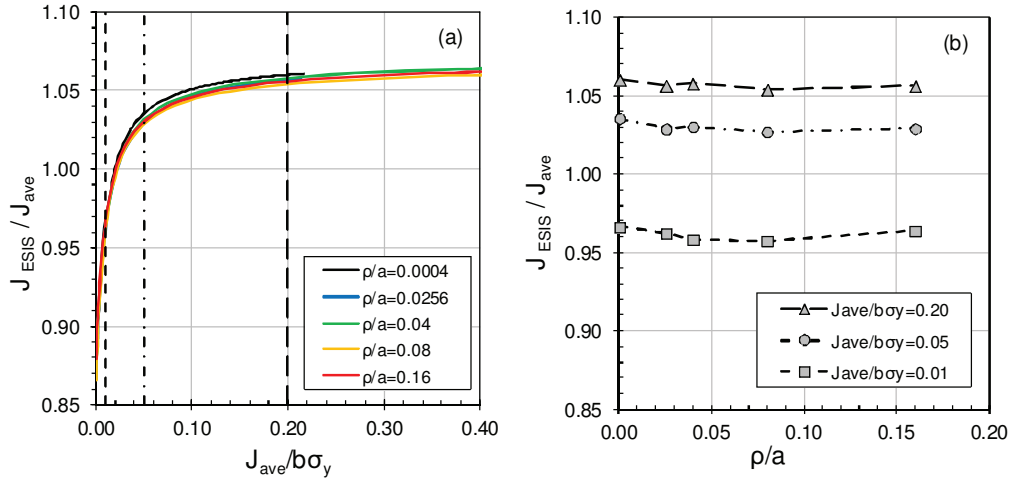


Figure 3: $J_{ESIS}$ / $J_{ave}$ for CT specimens as a function of (a) normalised $J_{ave}$ for various ρ/a, and (b) as a function of ρ/a for three normalised $J_{ave}$.

***Partitioned Solution ($J_{ASTM}$)***

Figure 4(a) shows the ratio of $J_{ASTM}$ to $J_{ave}$ plotted as a function of $J_{ave}/b\sigma_y$. As already noted, $J_{ASTM}$ is identical to $J_{BSI}$ for the CT specimen. The results indicate that there is a greater effect of ρ/a upon $J_{ASTM}$ than was observed on $J_{ESIS}$. The effect is also clear in Figure 4(b) where it is evident that ρ/a has a greater effect on $J_{ASTM}$ at low levels of loading. For example, at a loading level of $J_{ave}/b\sigma_y$=0.01, $J_{ASTM}$ underestimates $J_{ave}$ by around 10% for the bluntest notch radius modelled, ρ/a=0.16. However, noting that effective toughness generally increases with increasing ρ/a, it is unlikely that failure would occur from a specimen containing a blunt notch at such low loads. This is therefore unlikely to be of significance when measuring $J_{ave}$ at failure for specimens with blunt notches. Given that at higher loads, ρ/a only weakly affects the accuracy of $J_{ASTM}$, it is reasonable to conclude that $J_{ASTM}$ provides a sufficiently accurate method for estimating $J_{ave}$ for CT specimens containing notches up to ρ/a=0.16.

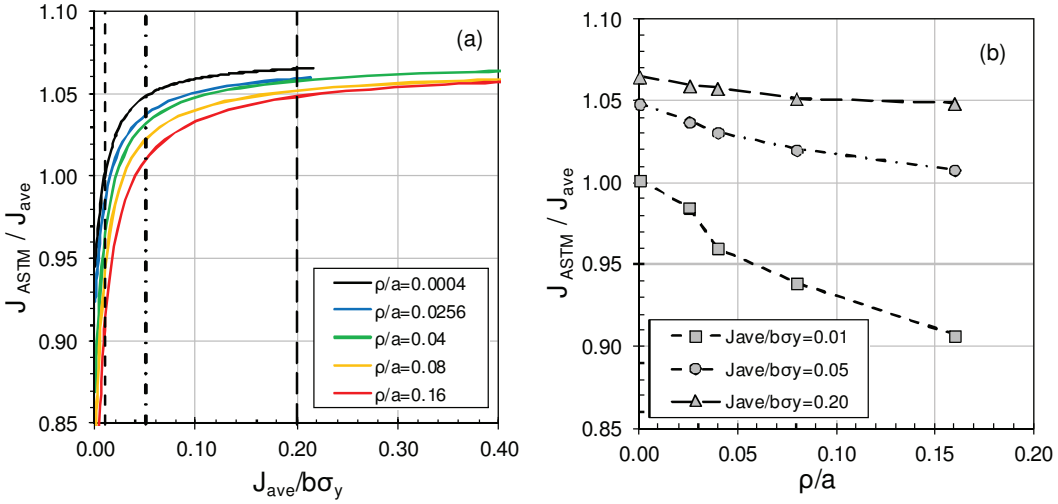


Figure 4: $J_{ASTM}$ / $J_{ave}$ for CT specimens as a function of (a) normalised $J_{ave}$ for various ρ/a, and (b) ρ/a for three normalised $J_{ave}$ values.

The FE models of the CT specimens were also analysed under plane strain conditions. This was achieved by additionally specifying $u_3$=0 boundary conditions on the two free surfaces normal to the plane of the notch. This approximated a 2D plane strain analysis but using the same 3D model as described previously. For this approximate 2D plane strain analysis, $J_{ave}$ was equal to each individual J-integral along the notch front.

The results in Figure 5 for the pre-cracked specimen under conditions of plane strain demonstrate that $J_{ASTM}$ provides an extremely good prediction, to within 1%, of $J_{ave}$ at all loading levels considered. This is indicative of the $J_{ASTM}$ solution having been derived from 2D plane strain analyses. For a 3D analysis where the J-integral reduces in magnitude along the crack front from the specimen centre towards the free surface, $J_{ave}$ is correspondingly lower than the J-integral in a 2D plane strain analysis. This leads to higher $J_{ASTM}/J_{ave}$ ratios in the 3D analyses, as observed in Figure 4.

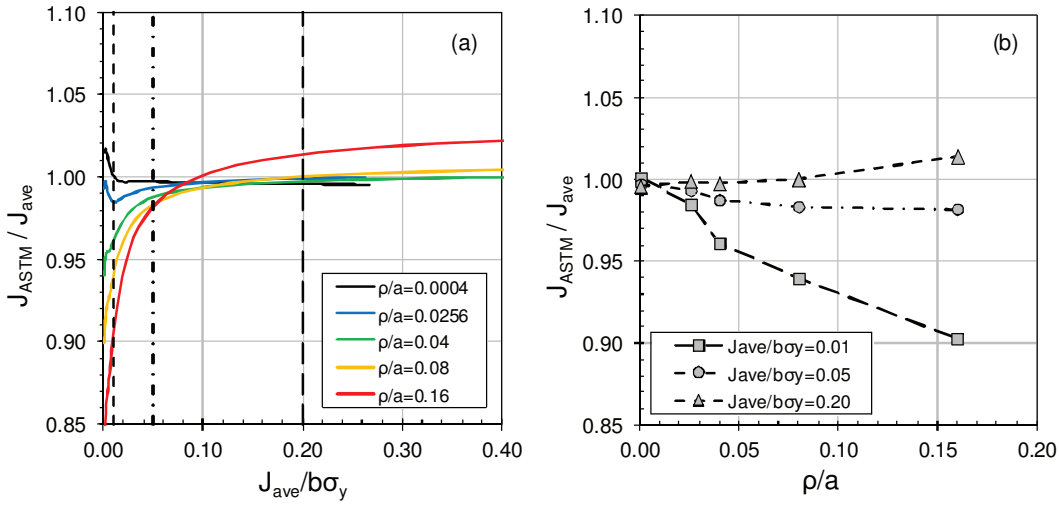


Figure 5: $J_{ASTM}/J_{ave}$ for CT specimens under plane strain conditions as a function of (a) normalised $J_{ave}$ for various ρ/a, and (b) as a function of ρ/a for three normalised $J_{ave}$ values.

For the notched specimens under conditions of plane strain, at low levels of loading, $J_{ASTM}$ underestimates $J_{ave}$ by up to 15% for ρ/a=0.16. However, at higher loading levels, $J_{ASTM}$ provides a significantly improved prediction of $J_{ave}$ for all ρ/a studied, to within 2.5%, and to within 1% for ρ/a≤0.08. These results imply that in plane strain, $J_{ASTM}$ is a very accurate predictor of $J_{ave}$ for notched specimens at all but very low levels of loading. At low loads, the errors in Figure 5 arise from the elastic component of J which is defined by K for a sharp crack. The use of K defined using sharp crack solutions introduces an error into $J_e$ for notches, and the effect of this error on the total J is more significant when $J_e$ dominates at low loads. At higher loads, the relative contribution from $J_e$ reduces, and hence the errors in J also reduce.

## RESULTS SUMMARY

The results shown above indicate that except at low loads, existing solutions (Equations 1 and 2) intended for measuring $J_{ESIS}$ and $J_{ASTM}$ in standard pre-cracked CT specimens provide reasonable estimates of $J_{ave}$ (to within around 6%) for notched CT specimens with root radii up to at least ρ/a=0.16. However, a common trend is that the estimates of $J_{ave}$ for notched specimens become less accurate at low loads. In order to summarise this effect, Figure 6 has been generated to show the minimum value of applied $J_{ave}$ required, as a function of ρ/a, to ensure the estimates of $J_{ave}$ are within 5% (Figure 6a) or 10% (Figure 6b). The results shown in Figure 6 can therefore be used as a simple tool to check whether the estimates provided by Equations 1 and 2 are likely to result in more significant errors.

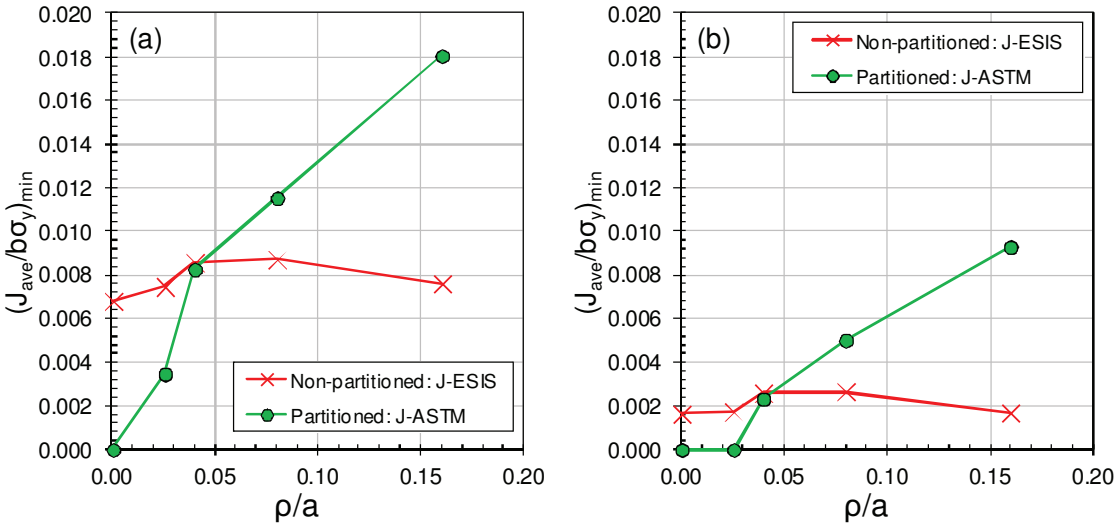


Figure 6: Minimum loading level required as a function of ρ/a to ensure that $J_{ave}$ in CT specimens is estimated to within (a) 5%, (b) 10%.

It is worth noting that critical values of J for notches with ρ/a=0.19 in Horn and Sherry (2010) have been measured to be around an order of magnitude greater than values for pre-cracked specimens. In an engineering context where uncertainties exist with respect to the notch root radius and the sensitivity of effective toughness to the notch radius, errors of less than 10% in the measurement of critical J values are likely to be small compared to uncertainties elsewhere in the overall structural integrity assessment.

Fracture toughness testing standards commonly impose validity limits to ensure that small scale yielding conditions prevail and that a single parameter, J, uniquely characterises the crack tip stress fields. When these validity limits are exceeded, small scale yielding conditions may no longer exist, and fracture toughness may increase due to the loss of crack tip constraint. Although the loss of crack tip constraint is not desirable for standard fracture toughness testing, testing under conditions of low crack tip constraint may be required when applying constraint-based assessments, and in these cases the validity limits are not relevant. However, the use of J alone is insufficient to describe fracture behaviour: additional parameters are required to describe the magnitude of crack tip constraint and its influence on the toughness of the material. The same logic applies when testing notched specimens: the validity limits designed to ensure small scale yielding conditions exist in pre-cracked specimens are not relevant. However, additional parameters must be used to describe the effect of the notch and its influence on the effective material toughness, such as those described in Cicero et al (2008) or Horn and Sherry (2012).

## CONCLUSIONS

The main general conclusions are as follows:

- Existing J solutions intended for pre-cracked CT specimens in ASTM E1820, BS7448-1 and ESIS P2-92 provide reasonably accurate estimates of $J_{ave}$ for notched test specimens, to within 10% in nearly all cases, and to within 5% in many cases.
- This is judged to be sufficiently accurate noting that in a FAD assessment of a structure containing a non-sharp defect, there will be other, potentially much larger, uncertainties relating to the defect tip radius and the dependence of effective toughness on notch radius.

- Although it is not considered necessary to propose new J solutions specifically for notched specimens, guidance has been provided as to when existing solutions are in error by more than 5 or 10% (typically under low loads).

The following specific conclusions provide additional details as to when more accurate estimates of $J_{ave}$ can be achieved.

- At high loads, existing J solutions provide reasonable estimates of $J_{ave}$ but can overestimate its value by up to 6%. These over-estimates are predominantly due to existing J solutions having been derived for plane strain conditions, whereas $J_{ave}$ is calculated from a three dimensional analysis.
- At very low loads, existing J solutions can underestimate $J_{ave}$ by over 15%. For partitioned J solutions, these under-estimates are due to errors in $J_e$ caused by the use of K defined for a sharp crack. The minimum loads necessary to achieve an estimate of within 5% and 10% are shown in Figure 6 (a) and (b) respectively.

## ACKNOWLEDGEMENTS

This paper is published with the permission of Amec Foster Wheeler and EDF Energy. The work was performed as part of the development programme for the EDF Energy R6 procedure.

## NOMENCLATURE

| | |
|---|---|
| $a$ | Crack or notch depth |
| $B$ | Specimen thickness |
| $b$ | Uncracked ligament ahead of the crack or notch |
| $E$ | Elastic modulus |
| $J$ | Elastic-plastic energy release rate |
| $J_e$ | Elastic component of $J$ |
| $J_p$ | Plastic component of $J$ |
| $J_{ave}$ | Weighted average of the J-integral along the crack/notch front |
| $J_{ASTM}$ | $J$ obtained from load-displacement data using ASTM E1820 |
| $J_{BSI}$ | $J$ obtained from load-displacement data using BS7448-1 |
| $J_{ESIS}$ | $J$ obtained from load-displacement data using ESIS P2-92 |
| $K$ | Linear elastic stress intensity factor |
| $L$ | Element size as defined in Figure 2 |
| $n$ | Strain hardening exponent |
| $r$ | Distance from the centre of curvature of the notch root radius |
| $U$ | Total area under load vs. displacement curve |
| $U_p$ | Plastic component of $U$ |
| $u_1, u_2, u_3$ | Displacement in the $x_1, x_2, x_3$ direction |
| $W$ | Specimen width |
| $x_1, x_2, x_3$ | Co-ordinate system |
| $\eta$ | Proportionality constant (Eq.1) |
| $\eta_p$ | Proportionality constant (Eq.2) |
| $\nu$ | Poisson's ratio |
| $\rho$ | Notch root radius |
| $\theta$ | Angle subtended at the centre of curvature of the notch radius |

| | |
|---|---|
| $\sigma_y$ | Yield stress defined at 0.2% plastic strain |
| CMOD | Crack Mouth Opening Displacement |
| CT | Compact Tension |
| FAD | Failure Assessment Diagram |
| FE | Finite Element |
| LLD | Load Line Displacement |
| SENB | Single Edge Notch Bend |

**REFERENCES**

ASTM (2011). "ASTM E1820-11: Standard Test Method for Measurement of Fracture Toughness". ASTM, Philadelphia, USA.

Brocks W. and Scheider I. (2003). "Reliable J Values: Numerical Aspects of the Path Dependence of J-Integral in Incremental Plasticity". 2003/22. GKSS, Geesthacht, Germany.

BSI (1991). "BS7448-1:1991. Fracture Mechanics Toughness Tests – Part I: Method for Determination of $K_{IC}$, CTOD and Critical J Values of Metallic Materials". BSI, London, UK.

BSI (2013). "BS7910:2013. Guide to Methods for Assessing the Acceptability of Flaws in Metallic Structures". BSI, London, UK.

Cicero S., Gutierrez-Solana F. and Alvarez J.A. (2008). "Structural Integrity Assessment of Components Subjected to Low Constraint Conditions". *Engineering Fracture Mechanics* 75 3038-3059.

ESIS (1992). "ESIS Procedure for Determining the Fracture Behaviour of Materials". ESIS, Delft, The Netherlands.

Horn A.J. and Budden P.J. (2015). "Development of Test Guidance for Single Edge Notch Bend Fracture Toughness Specimens Containing Notches Instead of Fatigue Pre-Cracks". *Proceedings of the ASME 2015 Pressure Vessels and Piping Conference, July 19-23, 2015, Boston, Massachusetts, USA*. PVP2015-45474.

Horn A.J. and Sherry A.H. (2010). "Prediction of Cleavage Fracture from Non-Sharp Defects Using the Weibull Stress Based Toughness Scaling Model". *International Journal of Pressure Vessels and Piping* 87 670-680.

Horn A.J. and Sherry A.H. (2012). "An Engineering Assessment Methodology for Non-Sharp Defects in Steel Structures – Part I: Procedure Development." *International Journal of Pressure Vessels and Piping* 89 137-150.

EDF Energy (2015). "R6 Revision 4. Assessment of the Integrity of Structures Containing Defects", latest updates: March 2015. EDF Energy, Gloucester, UK.